

*Communications in  
Applied  
Mathematics and  
Computational  
Science*

**ON A SCALABLE NONPARAMETRIC DENOISING  
OF TIME SERIES SIGNALS**

LUKÁŠ POSPÍŠIL, PATRICK GAGLIARDINI,  
WILLIAM SAWYER AND ILLIA HORENKO

vol. 13 no. 1 2018



## ON A SCALABLE NONPARAMETRIC DENOISING OF TIME SERIES SIGNALS

LUKÁŠ POSPÍŠIL, PATRICK GAGLIARDINI,  
WILLIAM SAWYER AND ILLIA HORENKO

Denoising and filtering of time series signals is a problem emerging in many areas of computational science. Here we demonstrate how the nonparametric computational methodology of the finite element method of time series analysis with  $H_1$  regularization can be extended for denoising of very long and noisy time series signals. The main computational bottleneck is the inner quadratic programming problem. Analyzing the solvability and utilizing the problem structure, we suggest an adapted version of the spectral projected gradient method (SPG-QP) to resolve the problem. This approach increases the granularity of parallelization, making the proposed methodology highly suitable for graphics processing unit (GPU) computing. We demonstrate the scalability of our open-source implementation based on PETSc for the Piz Daint supercomputer of the Swiss Supercomputing Centre (CSCS) by solving large-scale data denoising problems and comparing their computational scaling and performance to the performance of the standard denoising methods.

### 1. Introduction

Time series signals (i.e., data measured in intervals over a period of time) are typical for many practical areas such as econometrics (e.g., movement of stock prices [17]), climatology (e.g., temperature changes [39]), or molecular dynamics (e.g., in conformational changes of the molecule [19]). The analysis of time series signals aims to extract meaningful characteristics and understand the process which has generated those data. Such an analysis is the key ingredient in forecasting the process beyond the observed and measured time. However, one of the main difficulties in the analysis of real measurements is the presence of measurement/experimental noise. Additionally, an almost exponentially growing amount of collected data in many practical applications requires a development of better and faster data-driven denoising, modeling, and classification tools suitable for high performance computing (HPC).

---

*MSC2010:* 37M10, 62-07, 62H30, 65Y05, 90C20.

*Keywords:* time series analysis, quadratic programming, SPG-QP, regularization.

Suppose we observed time series signal  $x_t \in \mathbb{R}^n$ ,  $t = 1, \dots, T$ , (where  $n$  is the data dimension and  $T$  is the length of time series) and those data are appropriately described by the model function  $\mu(t, \Theta)$  with parameters  $\Theta \in \mathbb{R}^m$  and an additive noise  $\varepsilon$ , i.e.,

$$x_t = \mu(t, \Theta) + \varepsilon_t, \quad t = 1, \dots, T, \quad (1)$$

where  $\{\varepsilon_t\}$  is a family of independent and identically distributed (i.i.d.) random variables with zero expectation. The explicit model function  $\mu(t, \Theta)$  is chosen a priori based on our knowledge of the particular application. In general, the aim of the modeling process is to determine optimal parameters  $\bar{\Theta}$  such that the observed data  $x_t$  are described by (1) in the most optimal way, for example using maximum likelihood estimation (MLE) or minimizing mean-square error. Finally, the denoised signal can be obtained as an output of (1) with known  $\bar{\Theta}$  and without the presence of the (eliminated) noise term  $\varepsilon_t$ .

In the first part of the introduction, we shortly review the general classification of time series modeling methodologies based on the choice of  $\mu$ . In the second part, we investigate methods from the point of computational cost and highlight the importance of developing the optimization algorithms for effective solution. The final part of the introduction presents the finite element method of time series analysis with  $H_1$  regularization (FEM-H1) methodology used in the approach presented in this paper.

**1.1. General model classification.** In the simple case, the form of the model function  $\mu$  is known and, for instance, it can be expressed as some a priori defined function dependent on time. If the dimension of the underlying parameters  $\Theta$  is finite, then this method is called *parametric*.

For example, in the case of a linear regression

$$\mu(t, \theta_0, \theta_1) = \theta_1 t + \theta_0 \quad (2)$$

the unknown model parameters  $\theta_0, \theta_1 \in \mathbb{R}$  can be found using MLE (or minimizing least-square error) as a solution of an appropriate optimization problem

$$[\bar{\theta}_0, \bar{\theta}_1] = \arg \min_{\theta_0, \theta_1} \sum_{t=1}^T \|x_t - \mu(t, \theta_0, \theta_1)\|^2. \quad (3)$$

The recovered signal is obtained as values of  $\mu(t, \bar{\theta}_0, \bar{\theta}_1)$ ,  $t = 1, \dots, T$ . However, the model used (2) is valid only if the original data was generated by a linear model — and if no nonlinear effects had a significant impact on the underlying process.

Another example of parametric methods are hidden Markov models (HMMs). Here, it is a priori assumed that there exist regimes such that data in each regime is

distributed according to some explicit parametric distribution from a known and fixed family of parametric distributions (e.g., Gaussian, Poisson, etc.). The aim is then to search for an optimal regime-switching homogeneous Markov process represented by unknown components of transition matrix and initial states [1].

In general, parametric methods are usually based on rather strong explicit assumptions about the problem structure. These assumptions help create a tractable finite-dimensional formulation of the problem, which can be solved analytically or numerically and efficiently. In general, the more model assumptions are imposed, the less general the model is — and the simpler the numerical optimization problem to be solved is. On the other hand, imposing an unspecific parametric structure leads to models that incorrectly describe the problem under consideration.

The way to avoid the (possibly inappropriate) restrictive a priori explicit parametric assumptions about the dynamics of the model parameters is to use *nonparametric* models. In the case of nonparametric models, the dimension of the underlying parameters  $\Theta$  is infinite and we assume that optimal parameters are represented as functions from an a priori restricted class of feasible functions. However, the larger generality and complexity of the nonparametric models used also imposes a much higher computational cost on the resulting infinite-dimensional optimization problem. Therefore, the nonparametric models are much more challenging in numerical implementation and execution.

An example of a nonparametric method is a generalized additive model (GAM) [25]. In comparison to linear regression (2)–(3), the model function  $\mu$  in GAM can be defined as an arbitrary, nonlinear, and nonparametric smooth function from the Sobolev space on an interval  $[t_1, t_T] = [1, T]$

$$W^2([t_1, t_T]) = \left\{ \mu(\cdot) \in \mathcal{C}^{(2)}([t_1, t_T]) : \int_{t_1}^{t_T} [\mu''(\hat{t})]^2 d\hat{t} < \infty \right\}. \quad (4)$$

The optimal (i.e., sufficiently smooth) modeling function is then given by solving the optimization problem

$$\bar{\mu} = \arg \min \sum_{t=1}^T (x_t - \mu(t)) + \lambda \int_{t_1}^{t_T} [\mu''(\hat{t})]^2 d\hat{t}. \quad (5)$$

Here  $\lambda > 0$  represents the regularization parameter which has to be estimated [49].

**1.2. Computational cost.** Choosing the “most optimal” tools in every particular application is not a trivial task and is made more difficult by the interplay of many factors [36], most of all by the following two factors: (i) the amount of bias that is introduced by the analysis method (for example, coming from the eventually wrong a priori assumptions about the linearity, Gaussianity, and homogeneity of

the underlying processes) and (ii) the computational scalability of different data-driven algorithms — as well as the possibility to deploy these algorithms in an HPC setting — to be able to process the data en masse.

Experience shows that the analysis algorithms that introduce the highest-potential bias (e.g., standard linear Fourier filtering methods based on the fast Fourier transform (FFT) or parametric Bayesian methods like HMM with Gaussian or Poisson outputs and a time-homogenous Markov model assumption [36; 37; 47]) demonstrate the best HPC scaling performance whereas the nonlinear and non-Gaussian approaches like convolutional neural networks (CNNs) need more communication and scale worse — so only the deployment of massively parallel GPU architectures helped to reach the scale-up that was necessary to apply these methods to large realistic problems [11; 46].

From the mathematical perspective, essentially all of the data analysis and classification methods currently available in the standard analysis packages can be formulated as the numerical algorithms for solutions of large optimization problems.

To give some examples, the standard Fourier, wavelet, and kernel filtering algorithms for denoising the signals  $x_t \in \mathbb{R}^n$  — as well as the parameter identification methods for support vector machine (SVM) classification, linear discriminant analysis, and linear autoregressive models (AR) — can be formulated and implemented as solution algorithms for the same type of unconstrained quadratic minimization problem (QP)

$$\bar{y} = \arg \min_y \|x - \Phi y\|_2,$$

where  $\|\cdot\|_2$  denotes the Euclidean norm,  $y \in \mathbb{R}^r$  ( $r$  is typically much less than  $n$ ), and  $\Phi \in \mathbb{R}^{n \times r}$  is a known filtering matrix. Variational methods (like regularized kernel filtering, compressed sensing, and regularized model inference) [8; 50; 48] can be obtained by adding the regularizing inequality constraints to this convex problem: for example, a very popular compressed sensing algorithm in a dual formulation can be obtained by adding the linear inequality constraint  $\|y\|_1 \leq \epsilon$  (where  $\|\cdot\|_1$  denotes the  $L_1$  norm and  $\epsilon$  is some a priori fixed “sparsity” parameter) to the above unconstrained QP. Neural networks can be straightforwardly approached as parametric nonconvex optimization problems of the type

$$\bar{y} = \arg \min_y \|x - \Phi(y)\|_2,$$

where  $\Phi$  is some a priori fixed nonlinear operator characterizing the network topology and  $y$  are unknown network parameters.

Finally, the nonstationary and nonparametric denoising and modeling methods based on regularized nonconvex clustering algorithms (like the FEM-H1 methodology developed in [20]) can be implemented as the solution of a minimization problem

of a regularized clustering functional with equality and inequality constraints. In following we briefly review this approach.

**1.3. Nonparametric nonstationary FEM-HI methodology.** We will consider observed data as time series  $x_t \in \mathbb{R}^n$ ,  $t = 1, \dots, T$ . Our aim is to find coefficients  $\Theta(t)$  of some model function  $\mu(t, \Theta)$  such that this function in some sense fits the data in the best way. This fitting condition (i.e., the distance between observed data and values of the model function) is measured by a metric  $g$ , which can be for example defined by means of the function

$$g(x_t, \Theta(t)) = (x_t, \mathbb{E}[\mu(t, \Theta(t))])^2. \quad (6)$$

Therefore, the most appropriate parameters  $\Theta(t)$  can be obtained by solving the variational problem

$$\bar{\Theta} = \arg \min_{\Theta(\cdot) \in \Omega_{\Theta}} L(\Theta), \quad L(\Theta) = \sum_{t=1}^T g(x_t, \Theta(t)), \quad (7)$$

where  $L$  refers to a model distance function and  $\Omega_{\Theta}$  represents the space of all feasible parameters of parameter functions  $\Theta(\cdot)$  for the considered model. However, this problem is ill posed if only one sequence of data  $\{x_1, \dots, x_T\}$  is available (this is a typical situation for many practical applications, e.g., computational finance or climatology, where only one historical sequence of data is available for each particular time series). One option of regularizing this problem and making it well posed is based on the clustering of  $\Theta(t)$ ; i.e., one can assume that there exist  $K$  different stationary parameters  $\Theta = [\Theta_1, \dots, \Theta_K]$  such that the fitness function (6) can be expressed as a convex combination

$$g(x_t, \Theta(t)) = \sum_{i=1}^K \gamma_i(t) g(x_t, \Theta_i),$$

where  $\gamma_k(t) \in \{1, \dots, T\} \rightarrow [0, 1]$ ,  $k = 1, \dots, K$ , are so-called model indicator functions [38; 29]. These functions define the *activeness* of an appropriate  $i$ -th cluster at a given time  $t$ ; if  $\gamma_i(t) = 1$ , then the data are modeled by the  $i$ -th model in time  $t$ . These properties can be written in the form of constraints

$$\sum_{i=1}^K \gamma_i(t) = 1 \quad \text{for all } t, \quad 0 \leq \gamma_i(t) \leq 1 \quad \text{for all } t, i. \quad (8)$$

Hence, model indicator functions could be considered switching functions between individual models on clusters. Additionally, one can incorporate additional information about observed processes, for example by assuming that switching between clusters is in some sense slower than the changes of the signal caused by the presence

---

Set feasible initial approximation  $\Gamma^0 \in \Omega_\Gamma$

**while**  $\|L_\varepsilon(\Theta^k, \Gamma^k) - L_\varepsilon(\Theta^{k-1}, \Gamma^{k-1})\| \geq \varepsilon$   
 Solve  $\Theta^k = \arg \min_{\Theta \in \Omega_\Theta} L_\varepsilon(\Theta, \Gamma^{k-1})$  (with fixed  $\Gamma^{k-1}$ )  
 Solve  $\Gamma^k = \arg \min_{\Gamma \in \Omega_\Gamma} L_\varepsilon(\Theta^k, \Gamma)$  (with fixed  $\Theta^k$ )  
 $k = k + 1$

**end while**

Return approximation of model parameters  $\Theta^k$  and approximation of model indicator functions  $\Gamma^k$

---

**Algorithm 1.** Outer optimization algorithm.

of the modeling error or the noise in data. In our notation, this approach means that model indicator functions  $\gamma_i$  are smooth in some appropriately chosen function space. For example, one can enforce the smoothness in  $H_1$  space by introducing the Tikhonov-based penalization term

$$[\bar{\Theta}, \bar{\Gamma}] = \arg \min_{\substack{\Theta \in \Omega_\Theta \\ \Gamma \in \Omega_\Gamma}} L_\varepsilon(\Theta, \Gamma), \quad (9)$$

$$L_\varepsilon(\Theta, \Gamma) = \sum_{t=1}^T \sum_{i=1}^K \gamma_i(t) g(x_t, \Theta_i) + \varepsilon^2 \sum_{i=1}^K \sum_{t=2}^T (\gamma_i(t-1) - \gamma_i(t))^2,$$

where  $\Omega_\Gamma$  is a feasible set defined by conditions (8) and  $\varepsilon^2$  denotes the regularization parameter.

This methodology was called FEM-H1, and it was introduced and developed in [27; 28; 31; 29; 30; 32; 33]. For the unified and simplified derivation of the method, as well as its relation to classical methods of unsupervised learning, please see [38]. Moreover, the method was extended for spatial regularization using the network information in the graph-based form of the regularization matrix [20]. In this case, the only difference appears in the formulation of the smoothing term.

From a numerical point of view, the problem (9) can be solved as a sequence of split optimization problems; see Algorithm 1.

Please notice that the first optimization problem in Algorithm 1 is strongly connected to the type of modeling problem and model used. However, if we are able to solve the stationary variant of the problem, then this clustered problem includes only one modification represented by the multiplication by constant coefficients  $\gamma_i(t)$ . Beyond that, this problem can be reduced into  $K$  completely independent problems; for each cluster we are solving the stationary problem. And also the size of this problem is typically small since we suppose that the number of clusters is reasonably small.

One of the main challenges in applying this framework to the analysis of real time series data (e.g., in computational finance, climatology, or neuroscience) is the high



computational cost of the second optimization subproblem in this algorithm. Due to this limitation, published applications of these methods are confined to relatively small data sets [27; 28; 31; 29; 30; 32; 33]. This second optimization subproblem is completely independent of the type application, i.e., independent of the choice of fitness function (6). Nevertheless, the size of this problem is given by  $KT$  and cannot be separated because of the conditions (8) and the form of regularization term in (9). In optimization theory, the problem of this form (quadratic cost function with a feasible set formed by linear equality and inequality constraints) is called a quadratic programming problem (QP) [42; 14]. Therefore, if we develop the efficient solver to deal with this main computational bottleneck of the FEM-H1 data analysis framework, then we will be able to apply the framework to very large realistic data sets from different application areas (finance, image processing, bioinformatics, etc.). A central goal of this paper is to provide an algorithmic solution to this fundamental problem of the FEM-H1 framework.

Therefore, we will subsequently concentrate on the HPC solution of the problem of unknown model indicator functions  $\Gamma$ . For practical reasons, we define a column vector with all (unknown) model indicator functions by

$$\gamma := [\gamma_1, \dots, \gamma_K] \in \mathbb{R}^{KT}$$

and problem (9) for constant  $\Theta$  can be written in the form of block-structured QP problem

$$\begin{aligned} \bar{\gamma} &:= \arg \min_{\gamma \in \Omega_\Gamma} L_\epsilon(\gamma), \\ \gamma &:= [\gamma_1, \dots, \gamma_K] \in \mathbb{R}^{KT}, \\ \gamma_i &:= [\gamma_i(1), \dots, \gamma_i(T)] \in \mathbb{R}^T, \\ L_\epsilon(\gamma) &:= \frac{1}{T} b_\Theta^\top \gamma + \frac{\epsilon^2}{T} \gamma^\top H \gamma, \\ \Omega_\Gamma &:= \left\{ \gamma \in \mathbb{R}^{KT} : \gamma \geq 0 \wedge \sum_{k=1}^K \gamma_k(t) = 1 \text{ for all } t = 1, \dots, T \right\}, \end{aligned} \tag{10}$$

where  $H \in \mathbb{R}^{KT \times KT}$  is a block-diagonal matrix, whose blocks  $H_i \in \mathbb{R}^{T \times T}$  are formed by Laplace matrices, and

$$b_\Theta := [g(x_t, \Theta_1), \dots, g(x_t, \Theta_K)] \in \mathbb{R}^{KT}$$

denotes the column block-structured vector of modeling errors [29]. Notice that we scaled the cost function by positive coefficient  $1/T$  to control the scale of the function values for the cases with large  $T$ .

The paper is organized as follows. In Section 2, we examine the solvability and properties of the QP problem (10). Afterwards in Section 3, we present the modification of the spectral projected gradient method for QP problems suitable for an HPC implementation and discuss its advantages in comparison to other standard algorithms. In our project, we are interested in the HPC implementation of the FEM-H1 methodology to be able to deal with very long time series. From the beginning, we consider a situation when even the input data cannot be stored and operated on on one computational node; therefore, the distributed layout of the vectors and matrices has to be introduced and considered during the whole solution process. In Section 4 we briefly introduce our parallel implementation approach. Section 5 presents the performance of our algorithm on a data denoising problem, which is constructed to mimic the main features (like the very high noise-to-signal ratios and non-Gaussianity of the noise) that are typical for time series from practical applications. In contrast to the analysis of the “real life” practical data (where the underlying “true signal” is hidden in the noise and is not known a priori), analysis of this test data that we propose allows for a direct comparison of the introduced method to different standard denoising algorithms. It also allows the assessment of the denoising performance of the methods for various ratios of signal-to-noise — an assessment that cannot be achieved for the “real life” data. We also present the scalability results of our implementation on the Piz Daint supercomputer. In this section, we show the efficiency of FEM-H1 methodology in comparison with other standard denoising approaches. We show that our method outperforms other standard denoising methods in terms of the denoising quality in the situations when the signal-to-noise ratio of the data becomes small.

Finally, Section 6 concludes the paper and presents some ideas for our future research.

## 2. Solvability of inner QP

For the simplicity of our analysis, we rewrite the problem (10) using the convenient notation

$$\min_{x \in \Omega} f(x), \quad f(x) := \frac{1}{2}x^\top Ax - b^\top x, \quad (11)$$

where  $A := (\epsilon^2/T)H \in \mathbb{R}^{KT \times KT}$  is a symmetric positive semidefinite (SPS) Hessian matrix of a quadratic cost function  $f: \mathbb{R}^{KT} \rightarrow \mathbb{R}$  and  $b := -(1/T)b_\ominus^\top$  is the so-called right-hand side vector. This name came from the necessary optimality condition for the unconstrained problem  $\Omega = \mathbb{R}^{KT}$ , which is given by [42; 7; 14]

$$\nabla f(x) = Ax - b = 0 \iff Ax = b. \quad (12)$$

Since Hessian matrix  $A$  of the quadratic function  $f$  is SPS, this cost function is continuous and (not strictly) convex. Moreover, the null space (kernel) is given by

$$\text{Ker } A = \text{span}\{[\mathbf{1}^\top, \mathbf{0}, \dots, \mathbf{0}]^\top, [\mathbf{0}, \mathbf{1}^\top, \mathbf{0}, \dots, \mathbf{0}]^\top, \dots, [\mathbf{0}, \dots, \mathbf{0}, \mathbf{1}^\top]^\top\} \subset \mathbb{R}^{KT}, \quad (13)$$

where we denote  $\mathbf{1} := [1, \dots, 1]^\top \in \mathbb{R}^T$  and  $\mathbf{0} := [0, \dots, 0]^\top \in \mathbb{R}^T$ .

The feasible set  $\Omega \subset \mathbb{R}^{KT}$  is a (nonempty) bounded closed convex set, and it can be equivalently defined by

$$\Omega = \{\gamma \in \mathbb{R}^{KT} : \gamma \geq 0 \wedge B\gamma = c\},$$

where  $B := [I, \dots, I] \in \mathbb{R}^{T \times KT}$ ,  $c := \mathbf{1}$ , and  $I \in \mathbb{R}^{T \times T}$  denotes the identity matrix. Using this notation, we can easily conclude that the optimization problem (11) is a QP problem with the SPS Hessian matrix, linear equality constraints, and bound constraints

$$\min \frac{1}{2}x^\top Ax - b^\top x \quad \text{subject to } Bx = c, x \geq 0. \quad (14)$$

The existence of a solution of (14) is implied by the Weierstrass extreme value theorem: the real-valued cost function is continuous, and the nonempty feasible set is bounded.

However, the uniqueness of this solution is not so straightforward. It is given by the relationship between the null space (kernel) of Hessian matrix  $A$ , linear term  $b$ , and the feasible set  $\Omega$ , since the differences between solutions lies in this vector space. For instance, if  $A$  is symmetric positive definite (SPD), then the cost function is strictly convex and the solution is unique on any nonempty closed convex feasible set [14]. Unfortunately, in our case the Hessian matrix is only SPS and the solution is not unique for an arbitrary feasible set. For example in the unconstrained case, if  $\Omega := \mathbb{R}^n$ , then the problem could possibly be nonsolvable; if  $b \notin \text{Im } A$ , then the linear system (12) has no solution. If  $b \in \text{Im } A$ , then the system of all solutions of the unconstrained problem is given by  $\bar{x} = A^+b + d$ , where  $A^+$  denotes the Moore–Penrose pseudoinverse of the singular matrix  $A$  and the vector  $d$  represents an arbitrary vector from (in this case nontrivial)  $\text{Ker } A$ . Therefore, all solutions of the problem differ by the vector from  $\text{Ker } A$ .

At first, we present the generalization of previous observations from the unconstrained case to solutions of a problem (14).

**Lemma 1.** *Let  $\bar{x}_1, \bar{x}_2$  be two solutions of problem (14). Then*

$$\bar{x}_1 - \bar{x}_2 \in \text{Ker } A \cap \text{Ker } B.$$

*Proof.* Let us denote  $d := \bar{x}_2 - \bar{x}_1$ . Then using the definition of a quadratic cost function  $f$  and simple manipulations, we obtain

$$f(\bar{x}_2) = f(\bar{x}_1 + d) = f(\bar{x}_1) + d^\top \nabla f(\bar{x}_1) + \frac{1}{2}d^\top A d. \quad (15)$$

We suppose that both  $\bar{x}_1$  and  $\bar{x}_2$  are minimizers (both  $f(\bar{x}_1)$  and  $f(\bar{x}_2)$  are minimal values of  $f$  on the feasible set); therefore,  $f(\bar{x}_1) = f(\bar{x}_2)$ . Using this and comparing sides of equality (15), we can write

$$\frac{1}{2}d^\top A d = -d^\top \nabla f(\bar{x}_1). \quad (16)$$

The left side of this equation is always nonnegative because  $A$  is SPS. Moreover, the right side is nonpositive because  $\bar{x}_1$  is a solution of the convex optimization problem with differentiable  $f$  and the necessary optimality condition is given by [7]

$$\nabla f(\bar{x}_1)^\top (y - \bar{x}_1) \geq 0 \quad \text{for all } y \in \Omega.$$

Combining these two inequalities, we obtain

$$d^\top A d = 0 \wedge d^\top \nabla f(\bar{x}_1) = 0. \quad (17)$$

The first equality implies  $d \in \text{Ker } A$ .

We suppose that both of the solutions belong to the feasible set; therefore, they satisfy constraint conditions. From equality conditions for  $\bar{x}_2$  and using  $B\bar{x}_1 = c$ , we get

$$c = B\bar{x}_2 = B(\bar{x}_1 + d) = B\bar{x}_1 + Bd = c + Bd;$$

therefore,  $Bd = 0$  or equivalently  $d \in \text{Ker } B$ .  $\square$

In the proof of the previous lemma, we did not yet use one important property, which appears in (17). Using  $d \in \text{Ker } A$  from the first equality of (17), we get equivalent condition

$$d^\top \nabla f(\bar{x}_1) = d^\top (A\bar{x}_1 - b) = -d^\top b = 0$$

or equivalently (using  $d \in \text{Ker } A \cap \text{Ker } B$ ; see Lemma 1)

$$b \perp \text{Ker } A \cap \text{Ker } B.$$

This condition forms the sufficient condition for the possible existence of two different solutions of the general QP problem (14).

However, these solutions could be constrained by additional inequality constraints and the full system of necessary conditions is more complicated. Let us introduce a Lagrange function [42; 14] corresponding to the problem (14):

$$\mathcal{L}(x, \lambda_E, \lambda_I) := \frac{1}{2}x^\top A x - b^\top x + \lambda_E^\top (Bx - c) - \lambda_I^\top x, \quad (18)$$

where  $\lambda_I$  and  $\lambda_E$  are Lagrange multipliers corresponding to the equality and inequality constraints. So-called Karush–Kuhn–Tucker (KKT) optimality conditions

are given by

$$\begin{aligned}
 Ax - b + B^\top \lambda_E - \lambda_I &= 0, \\
 Bx - c &= 0, \\
 x, \lambda_I &\geq 0, \\
 [x]_j [\lambda_I]_j &= 0 \quad \text{for all } j = 1, \dots, KT,
 \end{aligned} \tag{19}$$

where we use the notation  $[v]_j$  to denote the  $j$ -th component of vector  $v$ .

Additionally, we can utilize the block-diagonal structure of our specific problem (10) given by the decomposition into clusters. Let us denote the block of matrix  $A$  by  $\hat{A} \in \mathbb{R}^{T \times T}$  and corresponding blocks of vectors  $x_k, b_k, \lambda_{Ik} \in \mathbb{R}^T, k = 1, \dots, K$ . Then we can write the first KKT system in a form

$$\hat{A}x_k - b_k + \lambda_E + \lambda_{Ik} = 0, \quad k = 1, \dots, K.$$

Now we can sum all these equations to get

$$\hat{A} \left( \sum_{k=1}^K x_k \right) - \sum_{k=1}^K (b_k + \lambda_{Ik}) + K\lambda_E = 0,$$

and since from the equality constraint we have  $\sum_{k=1}^K x_k = \mathbf{1}$  and  $\mathbf{1} \in \text{Ker } \hat{A}$  (see (13)), we can write

$$\lambda_E = \frac{1}{K} \sum_{k=1}^K (b_k + \lambda_{Ik}) \tag{20}$$

and substitute back into first KKT condition (19). Using the definition of a matrix  $B$ , we obtain

$$Ax - Qb - Q\lambda_I = 0, \quad Q := I - \frac{1}{K} B^\top B. \tag{21}$$

Here the orthogonal matrix  $Q \in \mathbb{R}^{KT \times KT}$  represents the projector onto  $\text{Ker } B$ .

Using KKT optimality conditions and the block structure of the problem, we are able to prove the following lemma, which gives the relationship between Lagrange multipliers corresponding to different solutions.

**Lemma 2.** *Let  $\bar{x}_1, \bar{x}_2$  be two different solutions of the problem (11) and let  $\bar{\lambda}_{1I}, \bar{\lambda}_{1E}, \bar{\lambda}_{2I}, \bar{\lambda}_{2E}$  be corresponding Lagrange multipliers in KKT system (19). Then*

$$\bar{\lambda}_{1I} = \bar{\lambda}_{2I} \quad \text{and} \quad \bar{\lambda}_{1E} = \bar{\lambda}_{2E}.$$

*Proof.* We have already shown that the Lagrange multipliers corresponding to equality constraints are uniquely given by the values of the Lagrange multipliers corresponding to the inequality constraints (20). Therefore, in the proof we will focus on a relationship between  $\bar{\lambda}_{1I}$  and  $\bar{\lambda}_{2I}$ .

Let us consider two different solutions  $\bar{x}_1$  and  $\bar{x}_2$ . These solutions satisfy all KKT conditions (19) and (21):

$$\begin{aligned} A\bar{x}_1 - Qb - Q\bar{\lambda}_{1I} &= 0, & A\bar{x}_2 - Qb - Q\bar{\lambda}_{2I} &= 0, \\ \bar{x}_1, \bar{\lambda}_{1I} &\geq 0, & \bar{x}_2, \bar{\lambda}_{2I} &\geq 0, \\ [\bar{x}_1]_j [\bar{\lambda}_{1I}]_j &= 0, & [\bar{x}_2]_j [\bar{\lambda}_{2I}]_j &= 0. \end{aligned}$$

Let us denote

$$\bar{x}_2 - \bar{x}_1 =: d, \quad \bar{\lambda}_{2I} - \bar{\lambda}_{1I} =: p \quad (22)$$

and substitute this into the first KKT condition for  $(\bar{x}_2, \bar{\lambda}_{2I})$ :

$$A(\bar{x}_1 + d) - Qb - Q(\bar{\lambda}_{1I} + p) = 0. \quad (23)$$

Since  $d \in \text{Ker } A$  (see Lemma 1) and using the first KKT condition for  $(\bar{x}_1, \bar{\lambda}_{1I})$ , we can write (23) in the form

$$Qp = 0 \implies p \in \text{Im } B^\top.$$

Now we focus on the inequality conditions. We use our notation (22) and substitute into KKT conditions (for all  $j = 1, \dots, KT$ ):

$$\begin{aligned} [\bar{x}_2]_j - [d]_j &\geq 0, & [\bar{x}_1]_j + [d]_j &\geq 0, \\ [\bar{\lambda}_{2I}]_j - [p]_j &\geq 0, & [\bar{\lambda}_{1I}]_j + [p]_j &\geq 0. \end{aligned}$$

We multiply these inequalities by nonnegative numbers  $[\bar{\lambda}_{2I}]_j, [\bar{\lambda}_{1I}]_j, [\bar{x}_2]_j, [\bar{x}_1]_j$  and use complementarity KKT conditions. We get

$$\begin{aligned} [d]_j [\bar{\lambda}_{2I}]_j &\leq 0, & [d]_j [\bar{\lambda}_{1I}]_j &\geq 0, \\ [p]_j [\bar{x}_2]_j &\leq 0, & [p]_j [\bar{x}_1]_j &\geq 0. \end{aligned}$$

Adding complementarity conditions with substitution (22) and using original complementarity conditions

$$\begin{aligned} -[d]_j [\bar{\lambda}_{2I}]_j - [p]_j [\bar{x}_2]_j + [d]_j [p]_j &= 0, \\ [d]_j [\bar{\lambda}_{1I}]_j + [p]_j [\bar{x}_1]_j + [d]_j [p]_j &= 0, \end{aligned}$$

we end up with

$$[d]_j [p]_j = 0 \quad \text{for all } j = 1, \dots, KT. \quad (24)$$

Let us remark that this condition is much stronger than  $d^\top p = 0$ , which could be obtained directly from

$$\begin{aligned} d &\in \text{Ker } A \cap \text{Ker } B, \\ p &\in \text{Im } B^\top, \end{aligned}$$

using  $\text{Ker } B \perp \text{Im } B^\top$  [35].

Now we are ready to prove that  $p = 0$ . Since  $p \in \text{Im } B^\top$ , there exists  $\alpha \in \mathbb{R}^T$  such that

$$p_k = \alpha \quad \text{for all } k = 1, \dots, K.$$

Suppose by contradiction that there exists an index  $i \in \{1, \dots, T\}$  such that  $[\alpha]_i \neq 0$ . Due to (24) corresponding components of  $d$  have to be zero, i.e.,

$$[d]_i = [d]_{i+T} = \dots = [d]_{i+(K-1)T} = 0. \quad (25)$$

However, if we suppose that  $d \neq 0$  (solutions  $\bar{x}_1$  and  $\bar{x}_2$  are different), then the vector  $d$  with property (25) is not from  $\text{Ker } A$  (see (13)), which is a contradiction. Therefore,  $p = 0$ .  $\square$

In the general case, we still cannot prove the uniqueness conditions. The following presents the situation when our problem (11) has an infinite number of solutions:

**Lemma 3.** *Let us consider the problem (11) with*

$$b \in \text{Im } B^\top$$

*and  $K \geq 2$ . Then this problem has an infinite number of solutions. Moreover, one of these solutions is given by*

$$\bar{x} = \frac{1}{K} \mathbf{1}. \quad (26)$$

*Proof.* At first, we prove that (26) is a solution. This point is not on the boundary of a feasible set; therefore, we can ignore the inequality constraints — all of them are satisfied and correspondingly  $\bar{\lambda}_I = 0$ . The first KKT condition (21) is given by

$$Ax = Qb.$$

Since  $Q$  is an orthogonal projector onto  $\text{Ker } B$  and we suppose  $b \perp \text{Ker } B$ , the right-hand side of this equation is equal to 0. Notice that  $\bar{x} \in \text{Ker } A$ ; therefore, the left-hand side is also equal to zero and the first KKT condition is satisfied. Moreover, the equality constraint could be also easily checked; therefore,  $\bar{x}$  is solution.

Now it remains to show that there exists at least one additional solution, i.e., that there exists a nonzero vector  $d \in \text{Ker } A \cap \text{Ker } B$  such that

$$\bar{x} + d \in \Omega.$$

Since we suppose  $K \geq 2$ , the vector space  $\text{Ker } A \cap \text{Ker } B$  is nontrivial and it is possible to choose a nonzero vector from this space. Additionally,  $\bar{x}$  does not belong to the boundary of  $\Omega$ ; therefore, there exists a nonzero vector in any *direction*.  $\square$

### 3. Spectral projected gradient method for QP problems

There exist several types of algorithms for solving a general QP problem (14). Since the manipulation with both constraint types is usually difficult, these algorithms are based on elimination of one type of constraint in the outer loop, and then they solve the sequence of inner problems with the remaining type of constraint.

To be more specific, one can use popular interior-point (IP) methods [42; 51]. These methods enforce the inequality constraints using a barrier function:

$$\min_{Bx=c, x \geq 0} f(x) \approx \min_{Bx=c} f(x) + \mu \sum_{i=1}^T \log x_i.$$

Here  $\mu > 0$  represents the barrier parameter. Using this approach, the algorithm transforms the original KKT system with inequalities (19) to the system of nonlinear equations with so-called duality gap  $\mu$ . The new problem is not equivalent to the original, but as the duality gap approaches zero, it becomes a better and better approximation. The barrier function increases all function values near the boundary of the feasible set to create an impenetrable barrier for a step-based algorithm which solves the inner problem with the remaining equality constraints. Usually  $\mu$  is not implemented as a constant but is a sequence  $\mu_k \rightarrow 0$ , and the solution of a previous inner problem is used as an initial approximation of the inner algorithm for a new  $\mu_{k+1}$ . Since the nonquadratic term (logarithm) is added to the original quadratic function  $f$ , the corresponding KKT system of this inner problem is nonlinear. To solve this system, one can use Newton-type methods with step size control to be sure that the new step will not jump through the barrier. Newton-type methods for solving nonlinear systems introduce the sequence of linear equations which have to be solved. For more details, see [42; 51].

Another approach is to deal with equality constraints first. This can be performed using augmented Lagrangian methods [42; 14]. The algorithm enforces the equality constraints using a penalty term:

$$\min_{Bx=c, x \geq 0} f(x) \approx \min_{x \geq 0} f(x) + \rho \|Bx - c\|^2.$$

Again, the new problem is not equivalent to the original one, although if  $\rho \rightarrow \infty$ , then  $\|Bx - c\| \rightarrow 0$ . Therefore, the penalty parameter  $\rho$  is usually implemented as the increasing sequence. The main advantage of this approach is the structure of the inner problem with inequalities — this new problem is again a QP. However, the Hessian matrix of the new problem is given by

$$\nabla^2(f(x) + \rho \|Bx - c\|^2) = A + \rho B^T B;$$



therefore, since the condition number depends on the value  $\rho$  and while  $\rho \rightarrow \infty$ , the problem becomes harder and harder to solve. Similar to the interior-point methods, there exists extensive theory about the connection between the stopping criterion for solving ill-conditioned inner problems and the value of a penalty parameter; see the semimonotonic augmented Lagrangian algorithm of [14] or [16]. The inner QP problem can be solved using the interior-point method, active-set algorithms, or projected gradient methods. In the case of bound constraints, the projection onto a feasible set is trivial. Therefore, in the case of the active-set algorithm and projected gradient methods, the inequality constraints are satisfied accurately, which is not the case for the interior-point methods. The barrier function makes it impossible to find the solution on the boundary of a feasible set, because in that case the value of a barrier term is equal to infinity.

This property brings us to the main disadvantage of both approaches. In the case of interior-point methods, it is impossible to satisfy inequality constraints accurately. In the case of the penalization technique, it is impossible to satisfy equality constraints exactly.

Fortunately, our QP problem (10) is not a general QP (14). To be more specific, the feasible set in our case is a separable set composed of  $T$  simplexes of size  $K$ . There exists an efficient algorithm for computing the projection of a general point onto simplex

$$P_{\Omega_t}(y) := \arg \min_{x \in \Omega_t} \|y - x\|,$$

$$\Omega_t := \left\{ \gamma_t \in \mathbb{R}^K : \gamma_t \geq 0 \wedge \sum_{k=1}^K [\gamma_t]_k = 1 \right\}, \quad t = 1, \dots, T,$$

$$\gamma_t := [\gamma_1(t), \dots, \gamma_K(t)]^\top.$$

The algorithm was presented in [10], and it computes the projection onto the simplex of dimension  $K$  in at most  $K$  steps; see Algorithm 2.

If we use these projections in our algorithm, all constraint conditions will be satisfied accurately. Moreover, computation of the projection can be performed as  $T$  independent processes, and since  $T$  is the largest parameter of problem dimension, this approach increases the granularity of the overall solution process — making it suitable for GPU computation. We can also use the value of the original cost function to stop our algorithm with respect to sufficient decrease given by demands from Algorithm 1.

Therefore, we are mainly interested in the projected gradient descent methods, i.e., in the algorithms which use  $x^0 \in \Omega$  as an initial approximation and suitable step lengths  $\alpha_k > 0$  to generate the approximations of the solution by

$$x^{k+1} = P_{\Omega}(x^k - \alpha_k \nabla f(x^k)), \quad k = 0, 1, \dots \quad (27)$$

---

Given arbitrary  $y \in \mathbb{R}^K$

**if**  $K = 1$  **then** set  $P(y) := 1$  and **stop**

Sort  $y$  in ascending order and set  $k := K - 1$

**while**  $k > 0$

$\alpha := (\sum_{j=k+1}^K [y]_j - 1) / (K - k)$

**if**  $\alpha > [y]_k$  **then**  $\hat{\alpha} := \alpha$  and  $k := -1$

**else**  $k := k - 1$

**end while**

**if**  $k = 0$  **then**  $\hat{\alpha} := (\sum_{j=1}^K [y]_j - 1) / K$

Set  $[P(y)]_k := \max\{[y]_k - \hat{\alpha}, 0\}$  for all  $k = 1, \dots, K$

Return  $P(y)$

---

**Algorithm 2.** Projection onto simplex [10].

In this case, the feasibility of generated approximations is enforced by using the projections, and the descent of the object function is induced by using  $-\nabla f(x)$ , which is generally the best local decrease direction. One of the most efficient projection gradient methods is a spectral projected gradient method (SPG) [5]. The first part of one SPG iteration is based on generating the point using (27) with step size defined by the Barzilai–Borwein algorithm (BB) [3]. However, the projected variant of BB is not convergent in general and the original proof of convergence cannot be applied [12] and an additional line-search technique has to be implemented.

In this section, we shortly review both components of SPG, i.e., the projected BB method and additional generalized Armijo condition. The method was developed to solve general optimization problems, and in this paper, we add our own modification for solving QP problems using the properties of the quadratic objective function.

Let us follow [45]. BB is the nonmonotone gradient descent method for solving unconstrained convex optimization problems. These methods are based on a construction of a sequence of solution approximations using the recursive formula

$$x^{k+1} = x^k - \alpha_k g^k, \quad k = 0, 1, \dots, \quad (28)$$

with a step size  $\alpha_k \in \mathbb{R}^+$  and a vector of steepest descent  $-g^k := -\nabla f(x^k)$ . The most popular gradient descent method is the steepest descent method (SD, first presented by Cauchy [9]). This method uses the step length, which minimizes the function  $f(x^{k+1})$  using locally optimal step size

$$\alpha_k = \arg \min_{\alpha \in \mathbb{R}} f(x^k - \alpha \nabla f(x^k)) = \frac{\langle g^k, g^k \rangle}{\langle A g^k, g^k \rangle}, \quad (29)$$

which leads to the monotone descent of the objective function.

However, the step size of BB is based on a different idea. To briefly review the relation of BB for the solution of unconstrained problems to Newton's method for solving a scalar nonlinear equation

$$g(x) = 0, \quad g : \mathbb{R} \rightarrow \mathbb{R},$$

let us replace the derivative  $g'(x^k)$  in Newton's method by its secant approximation to get

$$x^{k+1} = x^k - \frac{1}{g'(x^k)} g(x^k) \approx x^k - \frac{x^k - x^{k-1}}{g(x^k) - g(x^{k-1})} g(x^k). \quad (30)$$

Denoting  $g^k = g(x^k) = f'(x^k) = \nabla f(x^k)$  and

$$\alpha_k = \frac{x^k - x^{k-1}}{g^k - g^{k-1}}, \quad (31)$$

we can see that the secant method (30) can be considered as a gradient descent method (28). If  $g(x) : \mathbb{R}^n \rightarrow \mathbb{R}^n$ , then we cannot evaluate  $\alpha_k$  by (31), but we can assemble the *secant equation*

$$\frac{1}{\alpha_k} (x^k - x^{k-1}) = g^k - g^{k-1}. \quad (32)$$

After denoting

$$s^k = x^k - x^{k-1}, \quad g^k - g^{k-1} = As^k$$

and solving (32) in the least-square sense

$$\alpha_k = 1 / \arg \min_{\beta \in \mathbb{R}} (\langle s^k, s^k \rangle \beta^2 - 2 \langle As^k, s^k \rangle \beta + \langle As^k, As^k \rangle)$$

and some simplifications, we get

$$\alpha_k = \frac{\langle s^k, s^k \rangle}{\langle As^k, s^k \rangle}. \quad (33)$$

This is the step size of BB. The proof of convergence with estimates for solving the unconstrained QP problem (i.e., (14) with  $\Omega = \mathbb{R}^n$ ) was presented in [13].

However, the projected variant of BB (i.e., (27) with (33)) is not convergent in general and the original proof of convergence cannot be applied [12]. One option how to enforce the convergence of the method is to use an additional line-search. Let us denote the difference

$$g_{\alpha_k}^P(x^k) = P_{\Omega}(x^k - \alpha_k \nabla f(x^k)) - x^k \quad (34)$$

as a *projected gradient* at point  $x^k \in \Omega$  with the step length  $\alpha_k > 0$ . To enforce the convergence, the SPG algorithm uses an additional line-search step

$$x^{k+1} = x^k + \beta_k d_k \quad (35)$$

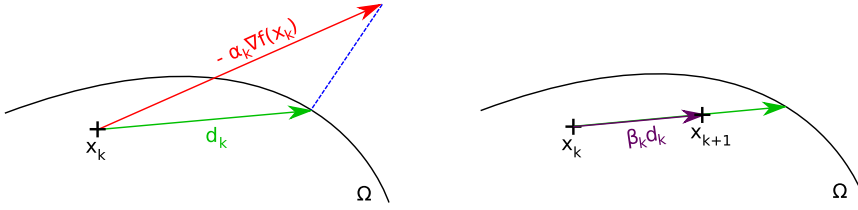


**Figure 1.** Projected gradient descent method with the additional line-search in two steps. Left: computation of projected gradient. Right: an additional line-search.

with  $d_k := g_{\alpha_k}^P(x^k)$  and an *appropriate* choice of the step size  $\beta_k \in (0, 1]$ . The method with these two steps (computation of the projected gradient and an additional line-search) is demonstrated in Figure 1.

The next lemma demonstrates the reason for using the projected gradient as a search direction in (35): it is a descent direction.

**Lemma 4.** *Let  $x \in \Omega$ ,  $\alpha > 0$ , and  $g_{\alpha}^P(x) = P_{\Omega}(x - \alpha \nabla f(x)) - x \neq 0$ . Then*

$$\langle g_{\alpha}^P(x), \nabla f(x) \rangle < 0. \quad (36)$$

*Proof.* We suppose  $\Omega \subset \mathbb{R}^n$  is a closed convex set; therefore [4],

$$\langle P_{\Omega}(y) - P_{\Omega}(z), y - z \rangle \geq \|P_{\Omega}(y) - P_{\Omega}(z)\|^2 \quad \text{for all } y, z \in \mathbb{R}^n.$$

If we choose  $y = x - \alpha \nabla f(x)$  and  $z = x = P_{\Omega}(x)$ , then we can estimate

$$\begin{aligned} -\alpha \langle g_{\alpha}^P(x), \nabla f(x) \rangle &= \langle g_{\alpha}^P(x), (x - \alpha \nabla f(x)) - x \rangle \\ &\geq \|g_{\alpha}^P(x)\|^2 > 0. \end{aligned} \quad \square$$

The SPG algorithm uses the Grippo–Lampariello–Lucidi method (GLL) [21] to find appropriate step size  $\beta_k$ . This algorithm is based on a bisection method to satisfy the so-called *generalized Armijo condition*

$$f(x^k + \beta_k d^k) < f_{\max} + \tau \beta_k \langle \nabla f(x^k), d^k \rangle. \quad (37)$$

Here  $\tau \in (0, 1)$  represents a safeguarding parameter and

$$f_{\max} := \max\{f(x^{k-j}) : 0 \leq j \leq \min\{k, m-1\}\}.$$

The main difference between this generalized version and the original Armijo conditions [42] is in the utilization of function values in  $m$  previous approximations instead of using only the previous  $f(x^{k-1})$ . This approach supplies the nonmonotonic behavior of BB and at the same time controls the descent. The proof of convergence of SPG is based on satisfying the generalized Armijo condition in every step [5]. We present SPG by Algorithm 3 and GLL by Algorithm 4.

Given cost function  $f : \mathbb{R}^n \rightarrow \mathbb{R}$ , initial approximation  $x^0 \in \Omega$ , projection onto feasible set  $P_\Omega(x)$ , safeguarding parameters  $0 < \alpha_{\min} \ll \alpha_{\max}$ , precision  $\varepsilon > 0$ , and initial step size  $\alpha_0 > 0$

```

k := 0
while  $\|P_\Omega(x^k - \nabla f(x^k)) - x^k\| > \varepsilon$ 
     $d^k := P_\Omega(x^k - \alpha_k \nabla f(x^k)) - x^k$ 
    Compute step size  $\beta_k$  using GLL
     $x^{k+1} := x^k + \beta_k d^k$ 
     $s^k := x^{k+1} - x^k$ 
     $y^k := \nabla f(x^{k+1}) - \nabla f(x^k)$ 
    if  $\langle s^k, y^k \rangle \leq 0$  then
         $\alpha_{k+1} := \alpha_{\max}$ 
    else
         $\alpha_{k+1} := \min\{\alpha_{\max}, \max\{\alpha_{\min}, \langle s^k, s^k \rangle / \langle s^k, y^k \rangle\}\}$ 
    end if
     $k := k + 1$ 
end while
Return approximation of solution  $x^{k+1}$ 
    
```

---

**Algorithm 3.** The original SPG method [6].

The main bottleneck of GLL is the computational complexity, which cannot be estimated in general. To be more specific, it is hard to say when the bisection will be finished.

The SPG was developed to solve more general optimization problems on convex sets. In our problems, the cost function is a quadratic function. We can use its particular form and its properties to simplify the GLL algorithm, obtaining an algorithm with fewer cost function evaluations, i.e., with a smaller number of the most time-consuming operations—multiplications by the Hessian matrix  $A$ . The motivation came from the other well known algorithms for solving QP, like the steepest descent method and the conjugate gradient method [26].

This modification was initially presented in [43], and it reduces the bisection in GLL to a simple formula.

First, let us present the basic equality in QP [14]: (for all  $x, d \in \mathbb{R}^n$  and  $b \in \mathbb{R}$ )

$$f(x + \beta d) = f(x) + \beta \langle Ax - b, d \rangle + \frac{1}{2} \beta^2 \langle Ad, d \rangle. \quad (38)$$

We start the simplification of SPG for solving QP problems with the most obvious simplifications. Notice that in the Algorithm 3 we can write

$$\begin{aligned} y^k &= \nabla f(x^{k+1}) - \nabla f(x^k) = (Ax^{k+1} - b) - (Ax^k - b) \\ &= A(x^{k+1} - x^k) = As^k. \end{aligned}$$

---

Given cost function  $f : \mathbb{R}^n \rightarrow \mathbb{R}$ , parameter  $m \in \mathbb{N}$ , approximation and direction  $x^k, d^k \in \mathbb{R}^n$ , parameter  $\tau \in (0, 1)$ , safeguarding parameters  $0 < \sigma_1 < \sigma_2 < 1$  for  $\sigma_1, \sigma_2 \in \mathbb{R}$

$$f_{\max} := \max\{f(x^{k-j}) : 0 \leq j \leq \min\{k, m-1\}\}$$

$$x_{\text{temp}} := x^k + d^k$$

$$\delta := \langle \nabla f(x^k), d^k \rangle$$

$$\beta := 1$$

**while**  $f(x_{\text{temp}}) > f_{\max} + \delta\beta\delta$

$$\beta_{\text{temp}} := -\frac{1}{2}\beta^2\delta/(f(x_{\text{temp}}) - f(x^k) - \beta\delta)$$

**if**  $\beta_{\text{temp}} \in \langle \sigma_1, \sigma_2 \rangle$  **then**

$$\beta := \beta_{\text{temp}}$$

**else**

$$\beta := \beta/2$$

**end if**

$$x_{\text{temp}} := x^k + \beta d^k$$

**end while**

Return step size  $\beta$

---

**Algorithm 4.** GLL line-search [21].

Since matrix  $A$  is SPS, we can write for any  $s^k \in \mathbb{R}^n \setminus \text{Ker } A$

$$\langle s^k, y^k \rangle = \langle s^k, As^k \rangle > 0,$$

and the condition in SPG (Algorithm 3) is always satisfied.

Moreover, the BB step length (33) is the inverse Rayleigh quotient (with  $s^k \notin \text{Ker } A$ ) and it can be bounded by

$$\frac{1}{\lambda_{\max}} \leq \alpha_{k+1} \leq \frac{1}{\hat{\lambda}_{\min}},$$

where  $\hat{\lambda}_{\min}$  is the smallest nonzero eigenvalue and  $\lambda_{\max}$  is the largest eigenvalue of the matrix  $A$  (in our case, the Hessian matrix is SPS; see (9) and (13)). Therefore, we can omit the safeguarding parameters  $\alpha_{\min}$  and  $\alpha_{\max}$  in Algorithm 3.

Let us take a better look into GLL line-search (Algorithm 4). The computation of  $\beta_{\text{temp}}$  can be simplified using (38). We obtain

$$\begin{aligned} \beta_{\text{temp}} &:= -\frac{\beta^2\delta}{2(f(x^k + \beta d^k) - f(x^k) - \beta\delta)} \\ &= -\frac{\beta^2\delta}{2\beta\delta + \beta^2\langle Ad^k, d^k \rangle - 2\beta\delta} = -\frac{\langle \nabla f(x^k), d^k \rangle}{\langle Ad^k, d^k \rangle} =: \bar{\beta}. \end{aligned}$$

This is a simple Cauchy step size (29). Since the vector  $d^k$  is the descent direction (36) and  $A$  is SPS, our optimal  $\bar{\beta}$  is positive. Obviously, the computation of a new  $\beta_{\text{temp}}$  is independent of the previous value and the original GLL method solely

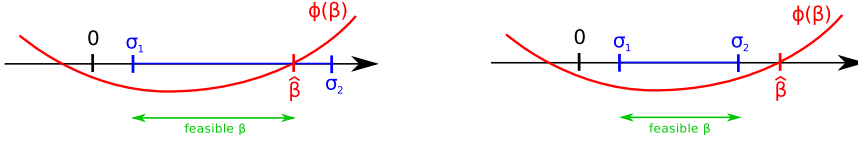


**Figure 2.** Possible situations in a GLL condition for QP.

performs the bisection method, i.e., tries to halve the coefficient  $\beta$  and verify the generalized Armijo condition. Furthermore, the value of a step size  $\beta$  has to be from the interval  $[\sigma_1, \sigma_2] \subseteq [0, 1]$ , because a smaller or larger value may cause a departure from the feasible set.

The division of step size  $\beta$  by 2 now modifies only the generalized Armijo condition. This condition can be also simplified as

$$\begin{aligned}
 0 &> f(x^k + \beta d^k) - f_{\max} - \tau \beta \delta \\
 &= f(x^k) + \beta \langle \nabla f(x^k), d^k \rangle + \frac{1}{2} \beta^2 \langle Ad^k, d^k \rangle - f_{\max} - \tau \beta \langle \nabla f(x^k), d^k \rangle \\
 &= \frac{1}{2} \beta^2 \langle Ad^k, d^k \rangle + (1 - \tau) \beta \langle \nabla f(x^k), d^k \rangle + f(x^k) - f_{\max}, \\
 0 &> \frac{1}{2} \beta^2 + (1 - \tau) \beta \frac{\langle \nabla f(x^k), d^k \rangle}{\langle Ad^k, d^k \rangle} + \frac{1}{\langle Ad^k, d^k \rangle} (f(x^k) - f_{\max}).
 \end{aligned}$$

Afterwards, we denote the function on the right-hand side and the constant term by

$$\Phi(\beta) := \frac{1}{2} \beta^2 - (1 - \tau) \bar{\beta} \beta - \xi, \quad \xi := \frac{1}{\langle Ad^k, d^k \rangle} (f_{\max} - f(x^k)).$$

We are interested in  $\beta$  such that the generalized Armijo condition in a form

$$\Phi(\beta) < 0 \tag{39}$$

is satisfied. The positive root of  $\Phi(\beta)$  is given by

$$\hat{\beta} := (1 - \tau) \bar{\beta} + \sqrt{(1 - \tau)^2 \bar{\beta}^2 + 2\xi}.$$

There exist only two possible situations; see Figure 2. Therefore, we can conclude that the feasible step size in the second step of SPG could be defined as

$$\beta_k \in [\sigma_1, \min\{\sigma_2, \hat{\beta}\}].$$

This simple interval can replace GLL; i.e., any  $\beta_k$  from this interval satisfies the generalized Armijo condition.

The computation of the function values can be also simplified using (38):

$$f(x^{k+1}) = f(x^k) + \beta_k \langle g^k, d^k \rangle + \frac{1}{2} \beta_k^2 \langle Ad^k, d^k \rangle.$$

---

Given cost function  $f : \mathbb{R}^n \rightarrow \mathbb{R}$ , initial approximation  $x^0 \in \Omega$ , projection onto feasible set  $P_\Omega(x)$ , parameters  $m \in \mathbb{N}$ ,  $\tau \in (0, 1)$ , safeguarding parameters  $0 < \sigma_1 < \sigma_2 < 1$  for  $\sigma_1, \sigma_2 \in \mathbb{R}$ , precision  $\varepsilon > 0$ , and initial step size  $\alpha_0 > 0$

```

k := 0
g0 := Ax0 - b
f0 :=  $\frac{1}{2} \langle g^0 - b, x^0 \rangle$ 
for k = 0, 1, ...
    dk := PΩ(xk - αkgk) - xk
    Compute matrix-vector multiplication Adk
    Compute multiple dot-product ⟨dk, {dk, Adk, gk}⟩
    if  $\sqrt{\langle d^k, d^k \rangle} \leq \varepsilon$  then stop
    fmax := max{f(xk-j) : 0 ≤ j ≤ min{k, m - 1}}
    ξ := (fmax - fk) / ⟨dk, Adk⟩
    β̄ := -⟨gk, dk⟩ / ⟨dk, Adk⟩
    β̂ := τβ̄ +  $\sqrt{\tau^2 \bar{\beta}^2 + 2\xi}$ 
    Choose βk ∈ ⟨σ1, min{σ2, β̂}⟩
    xk+1 := xk + βkdk
    gk+1 := gk + βkAdk
    fk+1 := fk + βk⟨dk, gk⟩ +  $\frac{1}{2} \beta_k^2 \langle d^k, Ad^k \rangle$ 
    αk+1 := ⟨dk, dk⟩ / ⟨dk, Adk⟩
    k := k + 1
end for
Return approximation of solution xk

```

---

**Algorithm 5.** SPG for QP problems (SPG-QP).

Finally, we can simplify the computation of the BB step length using (35) to

$$\alpha_{k+1} = \frac{\langle s^k, s^k \rangle}{\langle s^k, y^k \rangle} = \frac{\langle s^k, s^k \rangle}{\langle s^k, As^k \rangle} = \frac{\langle \beta_k d^k, \beta_k d^k \rangle}{\langle \beta_k d^k, \beta_k Ad^k \rangle} = \frac{\langle d^k, d^k \rangle}{\langle d^k, Ad^k \rangle}$$

and using the recursive formula for the computation of a new gradient:

$$g^{k+1} := Ax^{k+1} - b = A(x^k + \beta_k d^k) - b = g^k + \beta_k Ad^k.$$

We use all these simplifications to form Algorithm 5. For the sake of simplicity, we relabel the coefficient  $\tau := 1 - \tau \in (0, 1)$ .

Notice that the most time-consuming operation — multiplication by Hessian matrix  $A$  — is performed only once per iteration. Moreover, all scalar products in every iteration can be performed as a single operation. This feature decreases the amount of global communication during the solution process.



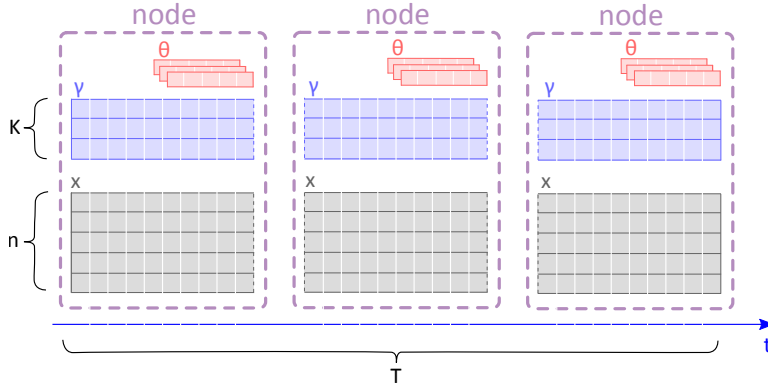


**Figure 3.** Large global vector of time series data  $X$  is distributed into nodes in a natural time-splitting way. Moreover, each node owns the part of global vector  $\gamma$  which corresponds to the time part of local data. Since the number of model parameters  $\Theta$  is small, each node owns its own local copy.

#### 4. HPC implementation

We are developing and maintaining a new HPC library [44] for nonstationary time series analysis in C++ using PETSc [2]. This library supports the manipulation of vectors distributed on multiple nodes. These data can be used during computation on CPUs or GPUs. Therefore, the user of our library can decide which architecture will be used for computation.

The solution of our problem consists of two different types of parallelization. The first type is straightforward: the problem (9) has to be solved for several values of regularization parameters  $\epsilon^2$  and various numbers of clusters  $K$ . Moreover, the solution obtained by the iterative process depends on an initial approximation. Each combination of these parameters can be used to run a completely independent instance of Algorithm 1. The parallelization in this case is *embarrassingly parallel*.

A more complicated parallelization scheme has to be used in a case where one instance of Algorithm 1 cannot be run on a single node, because of the size of the input data and/or the size of the unknowns, especially the size of vector  $\gamma$ . To deal with this problem, we naturally distribute the given long time series data  $X \in \mathbb{R}^{T \times n}$  into nodes as successive disjoint time subintervals with approximately the same size; see Figure 3.

Decomposition in time plays a key role in the effective computation of projections used in SPG-QP; see Algorithm 5. Using our approach, all data of one simplex are stored in one particular node; therefore, the projection is computed on each node fully independently. However, this decomposition in time brings new difficulties like disruption of diagonal-block structure of  $A$  defined in analysis in form (10); therefore, we had to implement an additional local-to-global index recomputation.

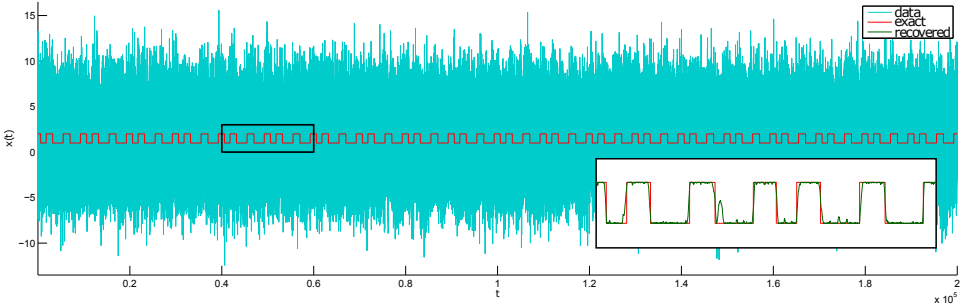


**Figure 4.** The beginning part of the benchmark signal of total length  $T = 10^7$ . Here the black box represents a part of the signal which is further enlarged to present the difference between the original signal (red) and the solution, namely the denoised signal (green). This denoised signal was obtained using optimal penalty parameter  $\varepsilon^2 = 3000$  (obtained with the standard L-curve method [22]) with norm of absolute error 0.04.

## 5. Numerical experiments

To demonstrate the scalability of our QP solver, we consider a time series  $K$ -means clustering problem. This problem is characterized by the most basic modeling functions: the piecewise-constant functions. We are trying to model the given data using the constant mean value in every cluster in least-square sense with the FEM-H1 regularization penalty in time:

$$\text{for all } t \in T_k, \quad x_t = \theta_k + \epsilon_t,$$

$$L_\varepsilon(\theta_1, \dots, \theta_K, \Gamma) = \sum_{t=0}^T \sum_{k=1}^K \gamma_k(t)(x_t - \theta_k)^2 + \varepsilon^2 \sum_{k=1}^K \sum_{t=0}^{T-1} (\gamma_{k,t+1} - \gamma_{k,t})^2.$$

As a benchmark, we take a short signal of length  $10^4$  and repeat this short signal to obtain long time series  $X_{\text{exact}}(t)$ . This long signal is considered to be an *exact* benchmark solution of our denoising algorithm. As an input of our problem we consider the signal with a variable noise  $\varepsilon$ :

$$X(t) = X_{\text{exact}} + \varepsilon, \quad \varepsilon \sim \mathcal{N}(0, 10). \quad (40)$$

Figure 4 presents a beginning part of the considered long signal of length  $T = 10^7$ .

We provide the exact parameter solution  $K = 2$ ,  $\theta_1 = 1$ ,  $\theta_2 = 2$  and solve the pure QP problem that represents the computational bottleneck of this time series denoising procedure. In SPG-QP, we choose  $\tau = 0.9$  and  $m = 20$  with respect to original SPG recommendations [5]. As a stopping criterion we choose the Euclidean norm of a projected gradient:

$$\|g^P(x)\| := \|P(x - \alpha \nabla f(x)) - x\| < 10^{-6}.$$

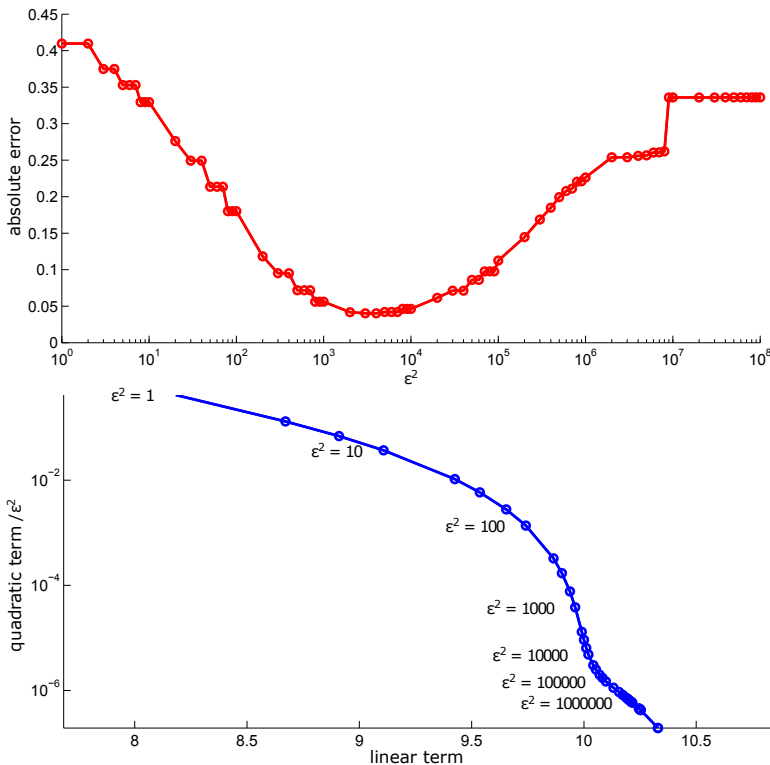


**Figure 5.** The mean value of  $L_1$  norm of absolute error for several values of penalty parameter (top). The left part of the graph represents the error which arises due to insufficient regularization, and the right part is caused by too much regularization, for the beginning part of benchmark signal of total length  $T = 10^7$ . The L-curve (bottom) presents the relation between values of the linear term (modeling error) and quadratic term (regularization) which depends on the choice of regularization parameter.

We implement Algorithms 1 and 5 in the PETSc framework and solve this problem for several values of penalty parameter  $\epsilon$ ; see Figure 5. Standard methods like L-curve [22] are then used to identify the optimal values for  $\epsilon$ . Based on these results, we choose value  $\epsilon = 3000$  for the following scalability tests.

To demonstrate the scalability of our implementation, we solve the abovementioned problem of parameters  $T = 10^7$ ,  $K = 2$ ,  $\epsilon^2 = 3000$  with  $\theta_1 = 1$  and  $\theta_2 = 2$  on CSCS Piz Daint using  $N \in \{1, 2, 4, 8, 16, 32, 64\}$  nodes. For complete specifications of this machine, see [http://www.cscs.ch/computers/piz\\_daint/](http://www.cscs.ch/computers/piz_daint/). For GPU computation, we run one MPI process per hybrid node (Intel Xeon E5-2690 v3 with NVIDIA Tesla P100), which uses the GPU for computation. In the case of CPU, we use pure CPU-nodes ( $2 \times$  Intel Xeon E5-2695, each with 18 cores) and run 36 MPI processes per node. PETSc deliberately chose not to support a multithreaded model, but rather only a multitask model (i.e., multiple MPI processes). Since we

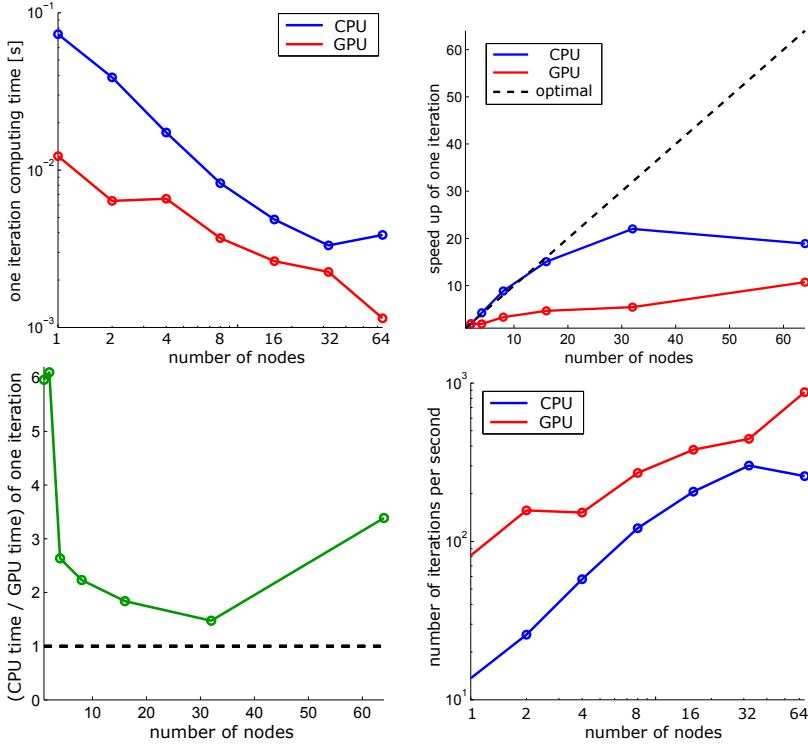


**Figure 6.** The strong scalability results: solution of QP problem of size  $2 \cdot 10^7$  on Piz Daint using different architectures — the computation time of one iteration (upper right), relative speed-up of computation time of one iteration (upper left), the number of iterations per second (lower left), and computation times on CPU and GPU (lower right).

are using PETSc, we are left with no choice and we do not use any CPU-thread parallelization (e.g., OpenMP) in our implementation.

We generated a time series signal of the length  $10^7$  and denoise it on different numbers of nodes. For statistical reasons, we decided to focus on the average numbers of QP iterations — where averaging was performed over different numbers of involved nodes. Please see the computation time of one iteration and number of iterations per second provided in Figure 6. Here we can observe good scalability of CPU for a small number of nodes. However, the problem is too small for larger number of CPUs or GPUs; therefore, the speedup is rapidly decreasing due to MPI communication. In all cases, the GPU computation is faster, but in this case, we should also consider the energy consumption; see Figure 7. These values were computed using the technique presented in [18].

Next, we would like to compare the introduced SPG-QP method for solving the inner QP problem with other existing HPC open-source implementations. The most straightforward choice is to use methods already implemented in PETSc,

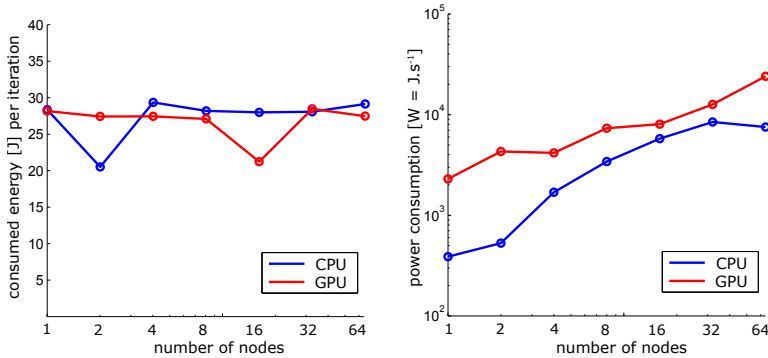


**Figure 7.** The energy consumption for one iteration of SPG-QP (left) and the power consumption (right).

for instance the Toolkit for Advance Optimization (TAO) [40]. However, for the combination of linear equalities and bound constraints (8), one can only use the interior-point method. Unfortunately, the actual manual pages say that the state-of-the-art implementation of the interior-point method in TAO is more of a placeholder for future constrained optimization algorithms and should not yet be used for large problems or production code. The most promising implementation of QP solvers in PETSc is PERMON (<http://permon.it4i.cz/>). The results for solving QP problems arising in linear elasticity contact problems [24] suggest good scalability performance and efficiency in the case of massively parallel CPU computation. However, our problem (10) has particular properties, especially the null spaces of the Hessian matrix and the matrix of linear equality constraints being not disjoint; see Lemma 1. Therefore, in our case the QP problem could have more than one solution. Besides that, we have tried to solve our problem with PERMON, but the algorithm is not able to solve problems with larger dimensions  $T > 10^4$ . Also the parameters of the algorithm have to be more precisely investigated and their tuning is nontrivial. Luckily, authors are working on generalization of the inner solver for solving the problems with singular Hessian matrices [15] and this approach should be implemented soon. Moreover, the GPU implementation is also future work. Summarizing these experiences, we were not able to find any QP solver that would be applicable to the particularly structured problem (10) of time series analysis — when the time series data is big (i.e., when  $T \gg 10^4$ ). For a complete survey of existing HPC QP libraries, see [23].

Next, we also compare the introduced FEM-H1 with implementations of standard denoising methods. We were not able to find any HPC open-source library which includes the HPC implementation of the denoising methods for time series on hybrid architectures. In our implementation, we decided to use PETSc for basic vector/matrix operations; therefore, we are directly able to switch between CPU/GPU

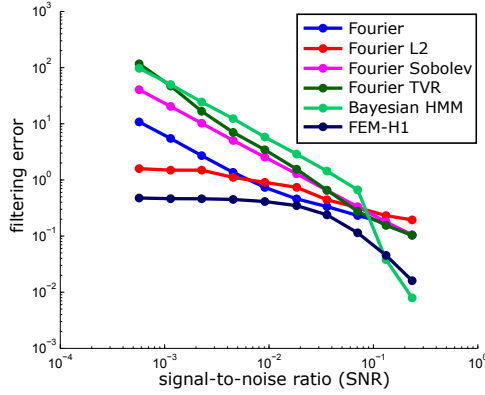


**Figure 8.** Dependence of the mean filtering error from the original signal-to-noise ratio (SNR). Results were obtained for the signal with Gaussian noise by averaging 100 independent realizations of the noisy signal data for each of the methods.

computations. Existing denoising libraries (e.g., Dlib C++ [34]) usually implement these operations from scratch using their own code, including basic vector/matrix operations, or (in the best case) use only sequential external BLAS libraries and cannot run on distributed memory architectures. Therefore, we decided to compare the denoising efficiency only for relatively short signals using the uniform sequential implementations in MATLAB [41]. To be more specific, we compare the following denoising algorithms.

- *Fourier* uses the MATLAB implementation of fft/iff and has one parameter  $s$ , which defines the size of the window.
- *Fourier  $L_2$*  is Fourier filtering with an additional  $L_2$  regularization term. There are two parameters:  $s$  as a size of the window and  $\lambda$  as a regularization parameter.
- *Fourier Sobolev* is Fourier filtering with an additional Sobolev prior penalty. This algorithm uses two parameters: size of the window  $s$  and regularization parameter  $\lambda$ .
- *Fourier TVR* is Fourier transformation with total variation regularization. The method leads to the system of nonlinear equations, which is typically solved using gradient method with constant step size and monotone descent of the solution error. The method uses three parameters: size of the window  $s$  and regularization parameters  $\lambda, \varepsilon$ .
- *Bayesian HMM* is the Bayesian hidden Markov model method [41]. This machine-learning algorithm uses random initial guesses; therefore, we run it 10 times and take the best solution with respect to the absolute error.

We have generated a large set of abovementioned testing signals of length  $T = 1000$ . For every standard deviation

$$\sigma \in 0.1 \cdot \{2, 8, 32, 128, 512, 2048, 8192, 32768, 131072, 524288\},$$

we generated 100 signals with random noise using formula (40) and then denoised the signal using the proposed algorithms. We set various algorithm parameters  $s \in \{5, 20, 30, 40, 60, 80\}$ ,  $\lambda \in \{0.1, 1, 10, 50, 100\}$ ,  $\varepsilon \in \{0.001, 0.01, 0.1\}$  and consider only the best solution with respect to the absolute norm computed as a difference between the denoised signal and the exact signal  $X_{\text{exact}}$ . Similarly for FEM-H1, we solved the problem for various values of penalty parameter.

At the end of the solution process, we computed the average absolute error value through all random noises. The results are presented in Figure 8. Here, the signal-to-noise ratio (SNR) was computed as the ratio of the maximum variation of the true signal to the maximum variation of the noisy signal.

As can be seen from Figure 8, FEM-H1 methodology outperforms the standard methods when the signal-to-noise ratio becomes smaller (i.e., when the noise is becoming larger as compared to the true underlying signal).

## 6. Conclusion

In this paper, we introduced an extension of the nonparametric FEM-H1 framework allowing it to be applied to denoising of very large time series data sets. We investigated basic properties of the inner large-scale QP subproblem — being the most expensive part of the FEM-H1 nonstationary time series analysis methodology. To solve this problem with HPC, we presented a modification of the spectral projected gradient method for QP problems. This method is based on projections, enjoys high granularity of parallelization, and is suitable to run on GPU clusters, such as Piz Daint at the Swiss Supercomputing Centre (CSCS). We presented numerical results for solving a large-scale time series denoising problem.

In future work, we will compare SPG-QP with state-of-the-art parallel implementations of popular optimization methods for solving not only benchmarks, but also solving problems in practical applications, such as the inference of causality networks from multiscale economical data. Additionally, our code will be extended by spatial regularization to increase the number of data analysis applications which could be practically solved by our emerging open-source HPC library.

## 7. Acknowledgments

This work is supported by the Platform for Advanced Scientific Computing (PASC) and financed by the PASC project “Towards the HPC-inference of causality networks from multiscale economical data” by Horenko, Gagliardini, and Sawyer. The work

of Horenko was partially supported by the Mercator Fellowship of the DFG SPP 1114 “Scaling cascades in complex systems”. We would like to gratefully thank Olga Kaiser, Dimitri Igdalov, Anna Marchenko, Benjamin Cumming, Patrick Sanan, Karl Rupp, Susanne Gerber, and the PERMON team (David Horák, Václav Hapla, et al.) for their collaboration in the project.

## References

- [1] N. Agmon, Y. Alhassid, and R. D. Levine, *An algorithm for finding the distribution of maximal entropy*, J. Comput. Phys. **30** (1979), no. 2, 250–258. Zbl
- [2] S. Balay, S. Abhyankar, M. F. Adams, J. Brown, P. Brune, K. Buschelman, L. Dalcin, V. Eijkhout, W. D. Gropp, D. Kaushik, M. G. Knepley, D. A. May, L. C. McInnes, K. Rupp, B. F. Smith, S. Zampini, H. Zhang, and H. Zhang, *PETSc*, users manual ANL-95/11, rev. 3.7, Argonne National Laboratory, 2016.
- [3] J. Barzilai and J. M. Borwein, *Two-point step size gradient methods*, IMA J. Numer. Anal. **8** (1988), no. 1, 141–148. MR Zbl
- [4] D. P. Bertsekas, *Nonlinear programming*, 2nd ed., Athena Scientific, 1999. MR Zbl
- [5] E. G. Birgin, J. M. Martínez, and M. Raydan, *Nonmonotone spectral projected gradient methods on convex sets*, SIAM J. Optim. **10** (2000), no. 4, 1196–1211. MR Zbl
- [6] ———, *Algorithm 813: SPG—software for convex-constrained optimization*, ACM Trans. Math. Softw. **27** (2001), no. 3, 340–349. Zbl
- [7] S. Boyd and L. Vandenberghe, *Convex optimization*, Cambridge University, 2004. MR Zbl
- [8] E. J. Candès and M. B. Wakin, *An introduction to compressive sampling*, IEEE Signal Proc. Mag. **25** (2008), no. 2, 21–30.
- [9] A.-L. Cauchy, *Méthode générale pour la résolution des systèmes d’équations simultanées*, Comptes Rendus Hebd. Séances Acad. Sci. **25** (1847), 536–538.
- [10] Y. Chen and X. Ye, *Projection onto a simplex*, preprint, 2011. arXiv
- [11] A. Coates, B. Huval, T. Wang, D. J. Wu, A. Y. Ng, and B. Catanzaro, *Deep learning with COTS HPC systems*, Proceedings of the 30th International Conference on Machine Learning (S. Dasgupta and D. McAllester, eds.), Proceedings of Machine Learning Research, no. 28, 2013, pp. 1337–1345.
- [12] Y.-H. Dai and R. Fletcher, *Projected Barzilai–Borwein methods for large-scale box-constrained quadratic programming*, Numer. Math. **100** (2005), no. 1, 21–47. MR
- [13] Y.-H. Dai and L.-Z. Liao, *R-linear convergence of the Barzilai and Borwein gradient method*, IMA J. Numer. Anal. **22** (2002), no. 1, 1–10. MR Zbl
- [14] Z. Dostál, *Optimal quadratic programming algorithms: with applications to variational inequalities*, Springer Optimization and Its Applications, no. 23, Springer, 2009. MR Zbl
- [15] Z. Dostál and L. Pospíšil, *Minimizing quadratic functions with semidefinite Hessian subject to bound constraints*, Comput. Math. Appl. **70** (2015), no. 8, 2014–2028. MR
- [16] ———, *Optimal iterative QP and QPQC algorithms*, Ann. Oper. Res. **243** (2016), no. 1–2, 5–18. Zbl
- [17] W. Enders, *Applied econometric time series*, 4th ed., Wiley, 2015.
- [18] G. Fourestey, B. Cumming, L. Gilly, and T. C. Schulthess, *First experiences with validating and using the Cray power management database tool*, Cray User Group proceedings, 2014.



- [19] S. Gerber and I. Horenko, *On inference of causality for discrete state models in a multiscale context*, Proc. Natl. Acad. Sci. USA **111** (2014), no. 41, 14651–14656. MR Zbl
- [20] ———, *Improving clustering by imposing network information*, Sci. Adv. **1** (2015), no. 7, 1500163.
- [21] L. Grippo, F. Lampariello, and S. Lucidi, *A nonmonotone line search technique for Newton’s method*, SIAM J. Numer. Anal. **23** (1986), no. 4, 707–716. MR Zbl
- [22] P. C. Hansen and D. P. O’Leary, *The use of the L-curve in the regularization of discrete ill-posed problems*, SIAM J. Sci. Comput. **14** (1993), no. 6, 1487–1503. MR Zbl
- [23] V. Hapla, *Massively parallel quadratic programming solvers with applications in mechanics*, Ph.D. thesis, Technical University of Ostrava, 2016.
- [24] V. Hapla, D. Horák, L. Pospíšil, M. Čermák, A. Vašatová, and R. Sojka, *Solving contact mechanics problems with PERMON*, High performance computing in science and engineering: second international conference (T. Kozubek, R. Blaheta, J. Šístek, M. Rozložník, and M. Čermák, eds.), Lecture Notes in Computer Science, no. 9611, Springer, 2015, pp. 101–115.
- [25] T. J. Hastie and R. J. Tibshirani, *Generalized additive models*, Monographs on Statistics and Applied Probability, no. 43, Chapman and Hall, 1990. MR Zbl
- [26] M. R. Hestenes and E. Stiefel, *Methods of conjugate gradients for solving linear systems*, J. Research Nat. Bur. Standards **49** (1952), 409–436. MR Zbl
- [27] I. Horenko, *On simultaneous data-based dimension reduction and hidden phase identification*, J. Atmos. Sci. **65** (2008), no. 6, 1941–1954.
- [28] ———, *On robust estimation of low-frequency variability trends in discrete Markovian sequences of atmospheric circulation patterns*, J. Atmos. Sci. **66** (2009), no. 7, 2059–2072.
- [29] ———, *Finite element approach to clustering of multidimensional time series*, SIAM J. Sci. Comput. **32** (2010), no. 1, 62–83. MR Zbl
- [30] ———, *On clustering of non-stationary meteorological time series*, Dynam. Atmos. Oceans **49** (2010), no. 2–3, 164–187.
- [31] ———, *On the identification of nonstationary factor models and their application to atmospheric data analysis*, J. Atmos. Sci. **67** (2010), no. 5, 1559–1574.
- [32] ———, *Nonstationarity in multifactor models of discrete jump processes, memory, and application to cloud modeling*, J. Atmos. Sci. **68** (2011), no. 7, 1493–1506.
- [33] ———, *On analysis of nonstationary categorical data time series: dynamical dimension reduction, model selection, and applications to computational sociology*, Multiscale Model. Simul. **9** (2011), no. 4, 1700–1726. MR Zbl
- [34] D. E. King, *Dlib-ml: a machine learning toolkit*, J. Mach. Learn. Res. **10** (2009), 1755–1758.
- [35] A. J. Laub, *Matrix analysis for scientists and engineers*, Society for Industrial and Applied Mathematics, 2005. MR Zbl
- [36] F. Lotte, M. Congedo, A. Lécuyer, F. Lamarche, and B. Arnaldi, *A review of classification algorithms for EEG-based brain–computer interfaces*, J. Neural Eng. **4** (2007), no. 2, R1.
- [37] J. H. Macke, M. Oppen, and M. Bethge, *Common input explains higher-order correlations and entropy in a simple model of neural population activity*, Phys. Rev. Lett. **106** (2011), no. 20, 208102.
- [38] P. Metzner, L. Putzig, and I. Horenko, *Analysis of persistent nonstationary time series and applications*, Commun. Appl. Math. Comput. Sci. **7** (2012), no. 2, 175–229. MR Zbl
- [39] M. Mudelsee, *Climate time series analysis: classical statistical and bootstrap methods*, 2nd ed., Atmospheric and Oceanographic Sciences Library, no. 51, Springer, 2014. MR Zbl

- [40] T. Munson, J. Sarich, S. Wild, S. Benson, and L. C. McInnes, *Toolkit for Advanced Optimization (TAO)*, users manual ANL/MCS-TM-322, rev. 3.5, Argonne National Laboratory, 2014.
- [41] K. Murphy, *Hidden Markov model (HMM) toolbox for Matlab*, 2005.
- [42] J. Nocedal and S. J. Wright, *Numerical optimization*, Springer, 1999. MR Zbl
- [43] L. Pospíšil, *Development of algorithms for solving minimizing problems with convex quadratic function on special convex sets and applications*, Ph.D. thesis, Technical University of Ostrava, 2015.
- [44] L. Pospíšil, I. Horenko, P. Gagliardini, and W. Sawyer, *PASC-inference: open-source HPC library of nonparametric Bayesian causality inference methods*, 2017.
- [45] M. Raydan M., *Convergence properties of the Barzilai and Borwein gradient method*, Ph.D. thesis, Rice University, 1991. MR
- [46] K. Simonyan and A. Zisserman, *Very deep convolutional networks for large-scale image recognition*, preprint, 2015. arXiv
- [47] F. Stimberg, M. Opper, G. Sanguinetti, and A. Ruttor, *Inference in continuous-time change-point models*, Neural Information Processing Systems Conference 2011 (J. Shawe-Taylor, R. S. Zemel, P. L. Bartlett, F. Pereira, and K. Q. Weinberger, eds.), Advances in Neural Information Processing Systems, no. 24, 2011, pp. 2717–2725.
- [48] L. A. Vese and C. Le Guyader, *Variational methods in image processing*, CRC, 2016. MR Zbl
- [49] G. Wahba, *Spline models for observational data*, CBMS-NSF Regional Conference Series in Applied Mathematics, no. 59, Society for Industrial and Applied Mathematics, 1990. MR Zbl
- [50] Y. Wiaux, L. Jacques, G. Puy, A. M. M. Scaife, and P. Vandergheynst, *Compressed sensing imaging techniques for radio interferometry*, Mon. Not. R. Astron. Soc. **395** (2009), no. 3, 1733–1742.
- [51] S. J. Wright, *Primal-dual interior-point methods*, Society for Industrial and Applied Mathematics, 1997. MR Zbl

Received June 20, 2017.

LUKÁŠ POSPÍŠIL: lukas.pospisil@usi.ch  
*Università della Svizzera italiana, Lugano, Switzerland*

PATRICK GAGLIARDINI: patrick.gagliardini@usi.ch  
*Università della Svizzera italiana, Lugano, Switzerland*

WILLIAM SAWYER: wsawyer@cscs.ch  
*Swiss National Supercomputing Centre, Lugano, Switzerland*

ILLIA HORENKO: horenkoi@usi.ch  
*Università della Svizzera italiana, Lugano, Switzerland*

# Communications in Applied Mathematics and Computational Science

msp.org/camcos

## EDITORS

### MANAGING EDITOR

John B. Bell  
Lawrence Berkeley National Laboratory, USA  
jbbell@lbl.gov

### BOARD OF EDITORS

Marsha Berger	New York University berger@cs.nyu.edu	Ahmed Ghoniem	Massachusetts Inst. of Technology, USA ghoniem@mit.edu
Alexandre Chorin	University of California, Berkeley, USA chorin@math.berkeley.edu	Raz Kupferman	The Hebrew University, Israel raz@math.huji.ac.il
Phil Colella	Lawrence Berkeley Nat. Lab., USA pcolella@lbl.gov	Randall J. LeVeque	University of Washington, USA rjl@amath.washington.edu
Peter Constantin	University of Chicago, USA const@cs.uchicago.edu	Mitchell Luskin	University of Minnesota, USA luskin@umn.edu
Maksymilian Dryja	Warsaw University, Poland maksymilian.dryja@acn.waw.pl	Yvon Maday	Université Pierre et Marie Curie, France maday@ann.jussieu.fr
M. Gregory Forest	University of North Carolina, USA forest@amath.unc.edu	James Sethian	University of California, Berkeley, USA sethian@math.berkeley.edu
Leslie Greengard	New York University, USA greengard@cims.nyu.edu	Juan Luis Vázquez	Universidad Autónoma de Madrid, Spain juanluis.vazquez@uam.es
Rupert Klein	Freie Universität Berlin, Germany rupert.klein@pik-potsdam.de	Alfio Quarteroni	Ecole Polytech. Féd. Lausanne, Switzerland alfio.quarteroni@epfl.ch
Nigel Goldenfeld	University of Illinois, USA nigel@uiuc.edu	Eitan Tadmor	University of Maryland, USA etadmor@cscamm.umd.edu
		Denis Talay	INRIA, France denis.talay@inria.fr

## PRODUCTION

production@msp.org

Silvio Levy, Scientific Editor

---

See inside back cover or [msp.org/camcos](http://msp.org/camcos) for submission instructions.

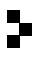
The subscription price for 2018 is US \$100/year for the electronic version, and \$150/year (+\$15, if shipping outside the US) for print and electronic. Subscriptions, requests for back issues from the last three years and changes of subscriber address should be sent to MSP.

Communications in Applied Mathematics and Computational Science (ISSN 2157-5452 electronic, 1559-3940 printed) at Mathematical Sciences Publishers, 798 Evans Hall #3840, c/o University of California, Berkeley, CA 94720-3840, is published continuously online. Periodical rate postage paid at Berkeley, CA 94704, and additional mailing offices.

---

CAMCoS peer review and production are managed by EditFLOW® from MSP.

PUBLISHED BY

 **mathematical sciences publishers**  
nonprofit scientific publishing

<http://msp.org/>

© 2018 Mathematical Sciences Publishers

# *Communications in Applied Mathematics and Computational Science*

vol. 13

no. 1

2018

- 
- |  |     |
|--|-----|
| Adaptively weighted least squares finite element methods for partial differential equations with singularities | 1   |
| BRIAN HAYHURST, MASON KELLER, CHRIS RAI, XIDIAN SUN and CHAD R. WESTPHAL                                       |     |
| On the convergence of iterative solvers for polygonal discontinuous Galerkin discretizations                   | 27  |
| WILL PAZNER and PER-OLOF PERSSON   |     |
| Theoretically optimal inexact spectral deferred correction methods   | 53  |
| MARTIN WEISER and SUNAYANA GHOSH   |     |
| A third order finite volume WENO scheme for Maxwell's equations on tetrahedral meshes                          | 87  |
| MARINA KOTOVSHCHIKOVA, DMITRY K. FIRSOV and SHIU HONG LUI  |     |
| On a scalable nonparametric denoising of time series signals   | 107 |
| LUKÁŠ POSPÍŠIL, PATRICK GAGLIARDINI, WILLIAM SAWYER and ILLIA HORENKO  |     |



1559-3940(2018)13:1;1-C